AEROELASTIC STABILITY OF WIND TURBINE BLADE/AILERON SYSTEMS

J. C. Strain, General Electric Co.
L. Mirandy, General Electric Co.

ABSTRACT

Aeroelastic stability analyses have been performed for the MOD-5A blade/aileron system. Various configurations having different aileron torsional stiffness, mass unbalance, and control system damping have been investigated. The analysis was conducted using a code recently developed by the General Electric Company - AILSTAB. The code extracts eigenvalues for a three degree of freedom system, consisting of: (1) a blade flapwise mode, (2) a blade torsional mode, and (3) an aileron torsional mode. Mode shapes are supplied as input and the aileron can be specified over an arbitrary length of the blade span. Quasi-steady aerodynamic strip theory is used to compute aerodynamic derivatives of the wing-aileron combination as a function of spanwise position. Equations of motion are summarized herein. The program provides rotating blade stability boundaries for torsional divergence, classical flutter (bending/torsion) and wing/aileron flutter. It has been checked out against fixed-wing results published by Theodorsen and Garrick.

The MOD-5A system is stable with respect to divergence and classical flutter for all practical rotor speeds. Aileron torsional stiffness must exceed a minimum critical value to prevent aileron flutter. The nominal control system stiffness greatly exceeds this minimum during normal operation. The basic system, however, is unstable for the case of a free (or floating) aileron. The instability can be removed either by the addition of torsional damping or mass-balancing the ailerons.

The MOD-5A design was performed by the General Electric Company, Advanced Energy Program Department under Contract DEN3-153 with NASA Lewis Research Center and sponsored by the Department of Energy.

INTRODUCTION

Although aileron systems have widespread use on fixed-wing aircraft very few rotors have been designed with aileron controls. Large wind turbines, in particular, have used pitchable blade sections for power regulation and to start-up and shut-down. General Electric's 400 ft. diameter, 7.3MW MOD-5A was originally designed with a pitchable tip spanning the outer 25% of blade radius. As the design progressed, further studies determined that substantial weight and cost savings could be obtained by switching to an aileron control system. This provided the impetus for the work described in this work.

In this paper we first describe the development of AILSTAB, a three degree of freedom stability analysis program. The results of the MOD-5A rotor blade stability analysis are then presented. Also included are the results of investigations, which are parametric in nature and show trends which should be similar for other WTG's.

NOMENCLATURE

a	-	distance, midchord to elastic axis, as percent of chord
$\bar{a}$	-	lift curve slope; lift coefficient per radian
b	-	semichord
c	-	distance, midchord to aileron hinge, as percent of chord
$c(k)$	-	Theodorsen's coefficient
C_A	-	elemental aerodynamic damping matrix
$\bar{C}_A$	-	integrated aerodynamic damping matrix
C_S	-	elemental structural damping matrix

PRECEDING PAGE BLANK NOT FILMED

$\bar{C}_S$ - integrated structural damping matrix

e - distance, midchord to leading edge of aileron, as percent of chord

h - blade flap bending degree of freedom

I_α - torsional moment of inertia of blade, less aileron, about elastic axis; per unit length

I_β - torsional moment of inertia of aileron, about hinge; per unit length

K_A - elemental aerodynamic stiffness matrix

$\bar{K}_A$ - integrated aerodynamic stiffness matrix

K_{CF} - elemental centrifugal stiffness matrax

$\bar{K}_{CF}$ - integrated centrifugal stiffness matrix

K_S - elemental structural stiffness matrix

$\bar{K}_S$ - integrated structural stiffness matrix

M_α - blade mass, less aileron; per unit length

M_β - aileron mass; per unit length

M_A - elemental aerodynamic mass matrix

$\bar{M}_A$ - integrated aerodynamic mass matrix

M_S - elemental structural mass matrix

$\bar{M}_S$ - integrated structural mass matrix

r - blade radial station, dimensional

S_h - Southwell coefficient, blade bending

V - local velocity

α - blade torsion degree of freedom

β - aileron torsion degree of freedom

ζ_h - critical damping ratio, blade bending

ζ_α - critical damping ratio, blade torsion

ζ_β - critical damping ratio, aileron torsion

ρ - air mass density; per unit length

σ_α - static moment of blade, less aileron, about elastic axis; per unit length

σ_β - static moment of aileron, about hinge; per unit length

ϕ_h - flapwise deflection mode shape

ϕ_α - blade torsion mode shape

ϕ_β - aileron torsion mode shape

$\phi_{\theta h}$ - flapwise rotation mode shape

Ω - rotor speed, radians/second

ω_f - flutter frequency, radians/second

ω_h - blade bending frequency, radians/second

ω_α - blade torsional frequency, radians/second

ω_β - aileron torsional frequency, radians/second

METHODS OF ANALYSIS

The AILSTAB rotor blade stability analysis program was developed in a manner very similar to that which would be used for a fixed wing. The differences between rotor and fixed wing analyses are the variation of local velocity with span on a rotor blade, and the variation of stiffness with rotor rpm due to the centrifugal forces. The AILSTAB computer code can be used to predict divergence and classical blade bending/torsion flutter, as well as aileron torsion/blade bending flutter.

SYSTEM DESCRIPTION

The three degrees of freedom (DOF) in the analysis are blade flapwise bending (h), blade torsion (α), and aileron torsion (β). Figure 1 depicts these DOF and their sign conventions. The conventions are such that h is negative for a bending deflection toward the suction side of the airfoil. α is positive for a "nose up" rotation, and β is positive for an "aileron down" rotation and is measured relative to α.

Three other parameters required for the analysis are depicted in this figure. All three are measured from the airfoil's midchord, are positive toward the trailing edge, and are expressed as a percentage of the semichord. The distance to the elastic axis is denoted "a", the distance to the aileron leading edge is "e", and the distance to the aileron hinge is denoted "c".

Figure 2 shows the three DOF (mode shapes) depicted in three dimensions.

ASSUMPTIONS

The following set of assumptions, all of which are believed to be reasonable, were made in developing the computer code.

1. The equations of motion were linearized.

2. Three degrees of freedom at a time, one flapwise, plus the blade and aileron torsion modes, are sufficient to determine the stability.

3. Aerodynamic strip theory with no stall was used, i.e. the aerodynamic derivatives are independent of α.

4. The local velocity is equal to Ωr, the rotational velocity times the radial distance, i.e. the free wind velocity is neglected.

5. The Theodorsen coefficient, c(k), is equal to 1.0, i.e. Quasi-steady aerodynamics are used. This should give conservative results for both blade-bending/torsion flutter and blade-bending/aileron torsion flutter.

6. Aerodynamic derivatives for an unsealed gap (ref. 1) are used if $c \neq e$.

EQUATIONS OF MOTION

The equations of motion were developed for a representative airfoil element of length "dr" and integrated along the span of blade with weighting as determined by the mode shapes. The aerodynamic equations incorporated in this analysis were those of Smilg and Wasserman (ref. 1). Inertial equations of motion were derived with centrifugal stiffening terms added. The final form of the equations is:

$$[\bar{M}_S - \bar{M}_A] \begin{Bmatrix} \ddot{h} \\ \ddot{\alpha} \\ \ddot{\beta} \end{Bmatrix} + [\bar{C}_S - \bar{C}_A] \begin{Bmatrix} \dot{h} \\ \dot{\alpha} \\ \dot{\beta} \end{Bmatrix} + [\bar{K}_S + \bar{K}_{CF} - \bar{K}_A] \begin{Bmatrix} h \\ \alpha \\ \beta \end{Bmatrix} = 0$$

where the matrices subscripted S (structural) and A (aerodynamic) are composed of elemental mass, damping, and stiffnes terms integrated along the blade span with modal weighting.

$$\text{i.e. } [\bar{M}_S] = \int_{\text{span}} L\phi_h \; \phi_\alpha \; \phi_\beta] \, [M_S] \begin{Bmatrix} \phi_h \\ \phi_\alpha \\ \phi_\beta \end{Bmatrix} dr$$

The stiffness contribution due to centrifugal stiffening, K_{CF}, is formed similarly with a mode shape of flapwise rotations substituted for the flapwise deflection mode shape.

$$\text{i.e. } [\bar{K}_{CF}] = \int_{\text{span}} L\phi_{\theta h} \; \phi_\alpha \; \phi_\varphi] \, [K_{CF}] \begin{Bmatrix} \phi_{\theta h} \\ \phi_\alpha \\ \phi_\beta \end{Bmatrix} dr$$

A detailed description of the terms in the elemental matrices is presented in the appendix.

SYSTEM STABILITY

In order to determine the blade's flutter stability, the integrated mass, stiffness and damping matrices are formed into a six by six dynamical matrix from which complex eigenvalues and eigenvectors are determined. The form of the dynamical matrix is:

$$\begin{bmatrix} -M^{-1}C & -M^{-1}K \\ I & 0 \end{bmatrix}$$

where

$$M = -\bar{M}_A + \bar{M}_S$$

$$C = -\bar{C}_A + \bar{C}_S$$

$$K = -\bar{K}_A + \bar{K}_S + \bar{K}_{CF}$$

$$I = 3 \times 3 \text{ unit matrix}$$

The critical damping ratios (ζ), and the frequencies in hz (f_f), are determined from the eigenvalue (R) as follows.

$$\zeta = -\frac{\text{REAL}(R)}{\text{ABS}(R)}, \qquad f_f = \frac{\text{ABS}(R)}{2\pi}$$

The output of the AILSTAB stability analysis program is eigenvalues, and eigenvectors if desired. The program is organized so that a series of cases may be run for a particular configuration, with rpm varied. The critical damping ratio and coupled frequencies are determined from the complex eigenvalues, and the damping in each mode can be plotted vs. rpm to illustrate system stability. In the case of blade bending/aileron tension flutter there is a range of rpm between which the instability exists. By plotting the range of unstable rpm vs. a design parameter such as aileron control system stiffness, aileron damper, or mass balance, a stability boundary may be constructed.

DESCRIPTION OF ANALYZED SYSTEM

The MOD-5A is a 7.2MW wind turbine with a teetered rotor. Ailerons on the outer 40% of the 200 ft. radius blades are used to regulate power and to shut down. The ailerons are hinged at their leading edge and are 40% of the chord width.

Three blade flapwise mode shapes were used in the

analysis. They were 1) the teeter mode with a frequency of 1 per rev, 2) the 1st collective with a frequency of 7 radians/second, and 3) the 1st cyclic with a frequency of 13.8 radians/second. These mode shapes were calculated for an isolated blade (i.e., not attached to the wind turbine). The collective mode of the isolated blade is found by providing a cantilevered root condition in the flapwise direction. The cyclic mode is determined by providing a pinned root condition in the flapwise direction. A plot of these three flapwise modes is presented in Figure 3. Southwell coefficients may be input to the program so that both the collective and cyclic frequencies may be varied with rpm to account for the varying centrifugal stiffening. For the MOD-5A analysis the important instability occurred at a low enough rpm so that the centrifugal stiffening was not important to the results.

The three aforementioned flapwise modes were each in turn analyzed in combination with the blade torsion mode shape and an aileron torsion mode. Higher modes than these were also analyzed, but were not found to be critical. The blade torsion mode had a frequency of 51 radians/second. By comparison, the ailerons are essentially rigid in torsion with cantilevered frequencies above 400 radians/second. For all practical purposes, the aileron natural frequencies are dominated by the control system stiffness and oscillate as a rigid body. Rather than attempting to model the actual aileron torsional natural mode, the frequency, or equivalently the actuator stiffness was varied, to determine the minimum requirements. In this way failure modes, such as loss of actuator hydraulic stiffness, are fall-outs of the analysis. In addition to aileron frequency sweeps, variations in aileron torsional damping, mass-balancing, and aileron spanwise length were considered. The ailerons center of gravity is aft of the 60% chord hinge line. The aft center of gravity has a de-stabilizing effect.

ANALYSIS RESULTS

The most critical condition will be discussed first. It occurs when the root torsional stiffness provided by the actuators is lost and the aileron is free to rotate about its hinges. This cannot happen under normal circumstances, so it represents a system failure. Stability boundaries are presented in terms of control system stiffness, control system damping, and the degree of mass-balance. A final case considers the stability of an aileron spanning only the outer 27.5% of the blade.

FREE AILERON

Figures 4a-c show damping vs. rotor speed for the baseline blade with a free, unbalanced aileron (the aileron torsion frequency of 1 per rev or 1P, is due to centrifugal stiffening). Below each damping curve, the natural frequencies are plotted vs. rpm. Both coupled (dashed lines) and uncoupled (solid lines) frequencies are shown. At rpm's where uncoupled frequencies coincide, a decrease in stability is noted in the corresponding damping curve. The Figures 4a, b, and c, illustrate the stability with the teeter, flap collective, and flap cyclic modes, respectively. Aileron torsion coupling is seen to cause an instability only with the flap collective mode. The ailerons are unstable in the region of low rotor speed, 3-12 rpm, which is typical of wing and aileron systems with an unbalanced mass. In particular, there is the possibility of instability when the aileron torsional frequency is less than the flapwise frequency. The system in Figure 4 becomes stable again at 12 rpm, because the torsional aerodynamic spring increases the aileron frequency beyond that of the first flapwise mode. The instabilities, which are seen in all plots between 55 and 60 rpm, are classical bending-torsion flutter of the blade.

STABILITY BOUNDARIES

A flutter boundary for the MOD-5A blade with unbalanced aileron is given in Figure 5. To generate the boundary, the aileron root torsion spring was increased in increments to find the stiffness at which the torsion mode became stable. At any value of stiffness where an instability occurred, the values of rpm between which the mode was unstable were found and plotted. This figure shows that an aileron torsional frequency of 7.5 radians/second is needed to provide neutral stability. This same procedure was followed for the addition of aileron torsional damping rather than a spring. The resulting flutter boundary is presented in Figure 6.

The comparison of stiffness and damping requirements is an interesting sidelight to the stability problem. If the damping rate is multiplied by the flutter frequency, the effective impedance, in stiffness units of the damper is found. Figure 7 contains plots of impedance vs. flutter damping ratio at 6 rpm for both spring and damper systems. The system's stability is largely a function of the aileron torsional impedance whether it be derived from a spring or a damper. This conclusion is further strengthened by Figure 8 which shows the stability boundaries in terms of impedances. The approximate equivalence of spring and damper impedance effects is an important consideration during dynamic conditions, such as pitch change in which the hydraulic actuator impedance has both spring and damper characteristics.

To prevent flutter without need for a mimimum aileron torsional stiffness or damper, balance weights would have to be added to the ailerons. With the ailerons unbalanced, the minimum damping ratio calculated in the AILSTAB rpm sweep was approximately -12%, as can be discerned from Figure 4b. The variation of modal damping with RPM is shown for a fully (100%) mass-balanced aileron in Figure 9. The system is stable. The variation of minimum damping in the aileron mode is shown for varying degrees of mass-balance in Figure 10. Neutral stability can be obtained with an 85% mass-balanced system.

EFFECT OF AILERON LENGTH

Similar analyses to those discussed above were performed with the free aileron section extending from .725 radius to the tip, rather than from .60 radius. In this configuration the different modal weighting caused an instability of the aileron coupling with the blade cyclic bending mode. Aileron torsion coupling with the blade collective bending mode also produced an instability, as it had with the longer aileron.

Since the shorter aileron was unstable in coupling with the higher frequency cyclic flapwise mode with a flutter frequency of approximately 14 radians/second, a higher dimensional damping coefficient was required to stabilize it. The longer aileron had unstable coupling only with the collective mode, which had a flutter frequency of approximately 7 radians/second.

The damping vs. rpm plots for the 27.5% span, free, unbalanced aileron analysis are presented in Figure 11.

Stability boundaries of rpm vs. aileron frequency are plotted in Figure 12 to show the effect of added root torsional stiffness. Boundaries for the addition of torsional damping are shown in Figure 13. To again demonstrate the similarity of results from adding impedance, whether from stiffness or damping, rpm vs. impedance stability boundaries are shown in Figure 14.

CONCLUDING REMARKS

The free unbalanced aileron caused the system to become unstable either with a length of 40% or of 27.5% of blade radius.

These instabilities can be removed with the addition of impedance to the aileron torsion degree of freedom. The actuator stiffness normally supplies an impedance well in excess of that required, but on the MOD-5A torsional dampers have been added to protect the system in the event of an actuator system failure. These dampers are passive elements which will always be operative. The damper forces far enough below those which are present due to the aerodynamic forces in normal operation so that their presence will not penalize control system design.

An alternate method of stabilizing the system would be through the addition of balance weights to the aileron. This method was deemed unwieldy and torsional dampers chosen instead.

REFERENCES

1. Scanlan, R.H. and Rosenbaum, R., "Aircraft Vibration and Flutter", MacMillan Co., 1951.

ACKNOWLEDGEMENTS

This work was performed by the General Electric Company under contract DEN 3-153 with NASA-Lewis Research Center. The authors would like to extend their thanks to David A. Spera and Timothy L. Sullivan of the NASA Wind Energy Project Office for their support throughout the program.

APPENDIX

Equations of Motion

STRUCTURAL (Left Hand Side)

$$[M_S]\begin{Bmatrix}\ddot{h}\\ \ddot{\alpha}\\ \ddot{\beta}\end{Bmatrix} + [C_S]\begin{Bmatrix}\dot{h}\\ \dot{\alpha}\\ \dot{\beta}\end{Bmatrix} + [K_S]\begin{Bmatrix}h\\ \alpha\\ \beta\end{Bmatrix} + [K_{CF}]\begin{Bmatrix}h\\ \alpha\\ \beta\end{Bmatrix}$$

$$\begin{aligned}
M_S(1,1) &= M_\alpha + M_\beta\\
M_S(1,2) &= \sigma_\alpha + \sigma_\beta + b\,(c-a)\,M_\beta\\
M_S(1,3) &= \sigma_\beta\\
M_S(2,2) &= I_\alpha + I_\beta + 2b\,(c-a)\,\sigma_\beta + b^2\,(c-a)^2\,M_\beta\\
M_S(2,3) &= I_\alpha + I_\beta + b\,(c-a)\,\sigma_\beta\\
M_S(3,3) &= I_\beta
\end{aligned}$$

Other structural mass terms are symmetric.

$$\begin{aligned}
C_S(1,1) &= 2\omega_h\,M_\alpha\,\zeta_h\\
C_S(2,2) &= 2\omega_\alpha\,I_\alpha\,\zeta_\alpha\\
C_S(3,3) &= 2\omega_\beta\,I_\beta\,\zeta_\beta
\end{aligned}$$

Other damping terms are zero.

$$\begin{aligned}
K_S(1,1) &= \omega_h^2\,M_\alpha + S_h\,\Omega^2\,M_S(1,1)\\
K_S(2,2) &= \omega_\alpha^2\,I_\alpha + \Omega^2\,M_S(2,2)\\
K_S(3,3) &= \omega_\beta^2\,I_\beta + \Omega^2\,M_S(3,3)
\end{aligned}$$

Other stiffness terms are zero.

The above structural mass, stiffness, and damping matrices are all multiplied by mode shapes at each radial station and integrated.

i.e.

$$\bar{M}_S = \sum_0^N [\phi_h\ \phi_\alpha\ \phi_\beta]^T\,[M_S]\,[\phi_h\ \phi_\alpha\ \phi_\beta]\,\Delta r$$

S_h in the above stiffness equation, is the southwell coefficient for the flapwise mode. It is an approximation used to relate the rotating and non-rotating blade natural frequencies.

$$\omega^2_{ROT} = \omega^2_{NON\text{-}ROT} + S_h\,\Omega^2$$

$$\begin{aligned}
K_{CF}(1,2) &= r\,\Omega^2\,M_S(1,2)\\
K_{CF}(1,3) &= r\,\Omega^2\,M_S(1,3)\\
K_{CF}(2,3) &= \Omega^2\,M_S(2,3)\\
K_{CF}(2,1) &= K_{CF}(1,2)\\
K_{CF}(3,1) &= K_{CF}(1,3)\\
K_{CF}(3,2) &= K_{CF}(2,3)
\end{aligned}$$

Diagonal terms are zero.

This centrifugal stiffness matrix is multiplied by mode shapes at each radial station and integrated. Unlike the structural stiffness matrix, the first row and column are multiplied by the modal rotation rather than deflection.

i.e

$$\bar{K}_{CF} = \sum_0^N [\phi_{\Theta h}\ \phi_\alpha\ \phi_\beta]^T\,[K_{CF}]\,[\phi_{\Theta h}\ \phi_\alpha\ \phi_\beta]\,\Delta r$$

Where, $\phi_{\Theta h} = \dfrac{d\phi_h}{dr}$

AERODYNAMIC (Right Hand Side)

$$[M_A]\begin{Bmatrix}\ddot{h}\\ \ddot{\alpha}\\ \ddot{\beta}\end{Bmatrix} + [C_A]\begin{Bmatrix}\dot{h}\\ \dot{\alpha}\\ \dot{\beta}\end{Bmatrix} + [K_A]\begin{Bmatrix}h\\ \alpha\\ \beta\end{Bmatrix}$$

$$\begin{aligned}
M_A(1,1) &= -\pi\,\rho\,b^2\\
M_A(1,2) &= \pi\,\rho\,ab^3\\
M_A(1,3) &= \rho\,(T_1 + (c-e)\,\phi_3)\,b^3\\
M_A(2,2) &= -\pi\,\rho\,(a^2 + 1/8)\,b^4\\
M_A(2,3) &= \rho\,[T_7 + (e-a)\,T_1 + 1/4\,(c-e)\,\phi_6\\
&\qquad - (a + 1/2)\,(c-e)\,\phi_3]\,b^4\\
M_A(3,3) &= \frac{\rho}{\pi}\,[T_5 + (c-e)\,\phi_{37} - (c-e)^2\,\phi_{17}]\,b^4
\end{aligned}$$

Other mass terms are symmetric.

$$C_A(1,1) = -\rho\,\bar{a}\,\Omega\,r\,b\,c\,(k)$$

$$C_A(1,2) = -1/2\,\rho\,\bar{a}\,\Omega\,r\,b^2 + \rho\,\bar{a}\,(a - 1/2)\,\Omega\,r\,b^2\,c\,(k)$$

$$C_A(1,3) = 1/2\,\frac{\rho}{\pi}\,\bar{a}\,T_4\,\Omega\,r\,b^2 + \frac{\rho}{\pi}\,\bar{a}\,[(c-e)\,\phi_1 - 1/2\,T_{11}]\,\Omega\,r\,b^2\,c\,(k)$$

$$C_A(2,1) = \rho\,\bar{a}\,(a + 1/2)\,\Omega\,r\,b^2\,c\,(k)$$

$$C_A(2,2) = 1/2\,\rho\,\bar{a}\,(a - 1/2)\,\Omega\,r\,b^3 + \rho\,\bar{a}\,(1/4 - a^2)\,\Omega\,r\,b^3\,c\,(k)$$

$$C_A(2,3) = \frac{\rho}{\pi}\,\bar{a}\,[P - 1/2\,(a - 1/2)\,T_4 + 1/2\,(c-e)\,\phi_5]\,\Omega\,r\,b^3$$

$$+ \frac{\rho}{\pi}\,\bar{a}\,[(a + 1/2)\,T_{11} - (a + 1/2)\,(c-e)\,\phi_1]\,\Omega\,r\,b^3\,c\,(k)$$
2

$$C_A(3,1) = \frac{\rho}{\pi}\,\bar{a}\,[(c-e)\,\phi_{31} - 1/2\,T_{12}]\,\Omega\,r\,b^2\,c\,(k)$$

$$C_A(3,2) = 1/2\,\frac{\rho}{\pi}\,\bar{a}\,[(c-e)\,\phi_{32} - (P - T_1 - 1/2\,T_4)]\,\Omega\,r\,b^3$$

$$+ \frac{\rho}{\pi}\,\bar{a}\,[1/2\,(a - 1/2)\,T_{12} + (1/2 - a)\,(c-e)\,\phi_{31}]\,\Omega\,r\,b^3\,c\,(k)$$

$$C_A(3,3) = 1/2\,\frac{\rho}{\pi^2}\,\bar{a}\,[1/2\,T_4\,T_{11} + (c-e)\,(\phi_{36} + \phi_{10}) - (c-e)^2\,\phi_{35}]\,\Omega\,r\,b^3$$

$$+ 1/2\,\frac{\rho}{\pi^2}\,\bar{a}\,[-1/2\,T_{11}\,T_{12} + (c-e)\,(\phi_2\,\phi_{31} + \phi_1\,\phi_8)$$

$$-2\,(c-e)^2\,\phi_1\,\phi_{31}]\,\Omega\,r\,b^3\,c\,(k)$$

$$K_A(1,1) = 0$$

$$K_A(1,2) = -\rho\,\bar{a}\,(\Omega\,r)^2 b\,c\,(k)$$

$$K_A(1,3)) = -\frac{\rho}{\pi}\,\bar{a}\,T_{10}\,(\Omega\,r)^2 b\,c\,(k)$$

$$K_A(2,1) = 0$$

$$K_A(2,2) = \rho\,\bar{a}\,(a + 1/2)\,(\Omega\,r)^2 b^2\,c\,(k)$$

$$K_A(2,3) = -1/2\,\frac{\rho}{\pi}\,\bar{a}\,[T_4 + T_{10}]\,(\Omega\,r)^2 b^2 + \frac{\rho}{\pi}\,\bar{a}\,(a + 1/2)\,T_{10}\,(\Omega\,r)^2 b^2\,c\,(k)$$

$$K_A(3,1) = 0$$

$$K_A(3,2) = +\frac{\rho}{\pi}\,\bar{a}\,((c-e)\,\phi_{31} - 1/2\,T_{12})\,(\Omega\,r)^2 b^2\,c\,(k)$$

$$K_A(3,3) = 1/2\,\frac{\rho}{\pi^2}\,\bar{a}\,[(c-e)\,\phi_{35} - (T_5 - T_4\,T_{10})]\,(\Omega\,r)^2 b^2$$

$$+ 1/2\,\frac{\rho}{\pi^2}\,\bar{a}\,[2\,(c-e)\,\phi_1\,\phi_{31} - T_{10}\,T_{12}]\,(\Omega\,r)^2 b^2\,c\,(k)$$

$$T_1 = -1/3 \sin(\cos^{-1}C)(2+C^2) + C\cos^{-1}C$$

$$T_3 = -(1/8+C^2)(\cos^{-1}C)^2 + 1/4\, C \sin(\cos^{-1}C)\cos^{-1}C(7+2C^2)$$

$$T_4 = -\cos^{-1}C + C \sin(\cos^{-1}C)$$

$$T_5 = -1 + C^2 - (\cos^{-1}C)^2 + 2C \sin(\cos^{-1}C)\cos^{-1}C$$

$$T_7 = -(1/8+C^2)\cos^{-1}C + 1/8\, C \sin(\cos^{-1}C)(7+2C^2)$$

$$T_{10} = \sin(\cos^{-1}C) + \cos^{-1}C$$

$$T_{11} = (\cos^{-1}C)\, C(1-2C) + \sin(\cos^{-1}C)(2-C)$$

$$T_{12} = \sin(\cos^{-1}C)(2+C) - \cos^{-1}C(2C+1)$$

$$P = -(\sin(\cos^{-1}C))^2\, 1/3$$

$$\phi_1 = \pi - \cos^{-1}(-e) + \sin(\cos^{-1}(-e))$$

$$\phi_2 = (\pi - \cos^{-1}(-e))(1-2e) + \sin(\cos^{-1}(-e))(2-e)$$

$$\phi_3 = \pi - \cos^{-1}(-e) - \sin(\cos^{-1}(-e))\, e$$

$$\phi_5 = \sin(\cos^{-1}(-e))(1+e)$$

$$\phi_6 = 2(\pi - \cos^{-1}(-e)) + \sin(\cos^{-1}(-e))\, 2/3\,(2+e)(1-2e)$$

$$\phi_8 = (\pi - \cos^{-1}(-e))(-1-2e) + \sin(\cos^{-1}(-e))(2+e)$$

$$\phi_{31} = \pi - \cos^{-1}(-e) - \sin(\cos^{-1}(-e))$$

$$\phi_{10} = \phi_{31}\, \phi_5$$

$$\phi_{17} = \phi_3^2 + [\sin(\cos^{-1}(-e))]^4$$

$$\phi_{32} = \pi - \cos^{-1}(-e) + \sin(\cos^{-1}(-e))(1+2e)$$

$$\phi_{35} = 2[\sin(\cos^{-1}(-e))]^2$$

$$\phi_{36} = \phi_{32}\, \phi_3 + 2[\sin(\cos^{-1}(-e))]^4$$

$$\phi_{37} = \phi_3(\phi_2 - \phi_3)$$

The aerodynamic mass, damping, and stiffness matrices are all multiplied by their mode shapes at each radial station and integrated.

i.e.

$$\bar{M}_A = \sum_0^N [\phi_h\, \phi_\alpha\, \phi_\beta]^T [M_A]\, [\phi_h\, \phi_\alpha\, \phi_\beta]\, \Delta r$$

DIVERGENCE

Torsional divergence, if present, will show up in the roots of the stability equations. The following has been added so that the divergence speed, which often lies beyond the RPM range of interest, may be computed directly.

To determine the blade's divergence speed the square of the rotational rotor velocity, Ω^2, must be factored out of the lower-right-hand 2 x 2 partition of the integrated aerodynamic stiffness matrix, $\bar{K}_A$. The same partition is factored out of the structural stiffness matrix $\bar{K}_S$ (the Southwell coefficient terms were ignored here). The two resulting partitions are then set equal to each other and the characteristic equation solved as shown below.

$$K_A' = \begin{bmatrix} \bar{K}_A(2,2) & \bar{K}_A(2,3) \\ \bar{K}_A(3,2) & \bar{K}_A(3,3) \end{bmatrix} \cdot \frac{1}{\Omega^2}$$

$$K_S' = \begin{bmatrix} \bar{K}_S(2,2) & \bar{K}_S(2,3) \\ \bar{K}_S(3,2) & \bar{K}_S(3,3) \end{bmatrix}$$

$$\begin{vmatrix} K_S'(1,1) - K_A'(1,1)\,\Omega^2 & K_S'(1,2) - K_A'(1,2)\,\Omega^2 \\ K_S'(2,1) - K_A'(2,1)\,\Omega^2 & K_S'(2,2) - K_A'(2,2)\,\Omega^2 \end{vmatrix} = 0$$

$$K_S'(2,1) = K_S'(1,2) = 0.$$

Expanded, the resulting equation is:

$$\Omega^4 \left(k_A'(1,1)\, K_A'(2,2) - K_A'(1,2)\, K_A'(2,1)\right)$$

$$-\Omega^2 \left(K_S'(2,2)\, K_A'(1,1) + K_S'(1,1)\, K_A'(2,2)\right) + K'_S(1,1)\, K'_S(2,2) = 0.$$

which is easily solved for Ω, the flutter speed in radians/second.

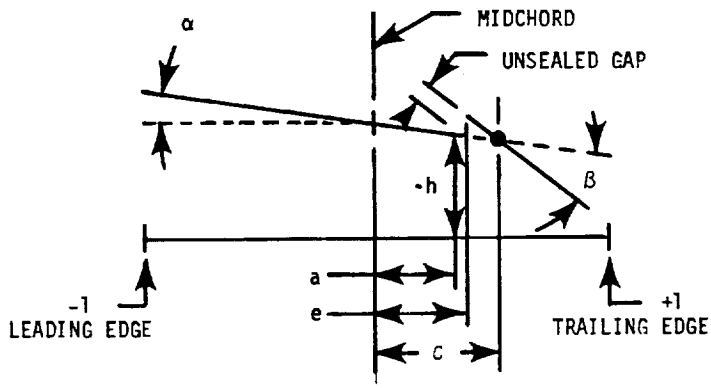

a	=	DISTANCE - MIDCHORD TO ELASTIC AXIS
e	=	DISTANCE - MIDCHORD TO AILERON L/E
c	=	DISTANCE - MIDCHORD TO AILERON HINGE
h	=	BLADE FLAPWISE DEFLECTION
α	=	BLADE TORSION ANGLE
β	=	AILERON TORSION ANGLE w.r.t.

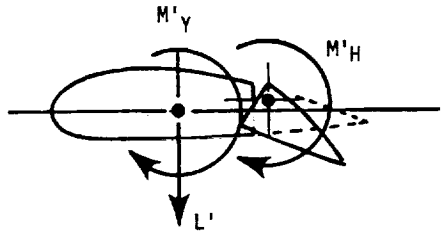

L'	=	RUNNING LIFT FORCE - POSITIVE POINTING FROM SUCTION SIDE TOWARD PRESSURE SIDE AS DEFINED IN REFERENCE 1
M'_Y	=	RUNNING MOMENT ABOUT ELASTIC AXIS
M'_H	=	RUNNING AILERON HINGE MOMENT

Figure 1. Sign Conventions and Terminology

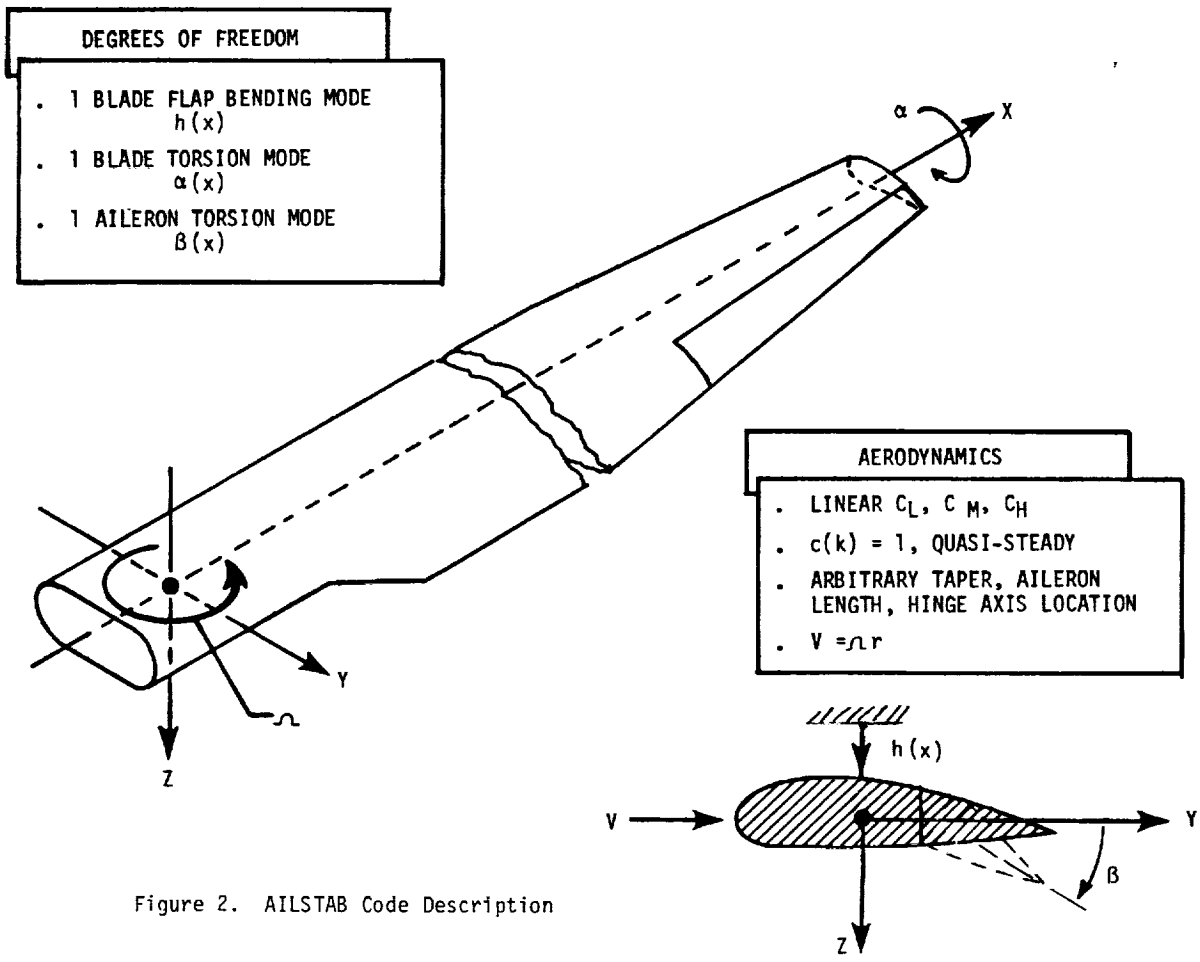

Figure 2. AILSTAB Code Description

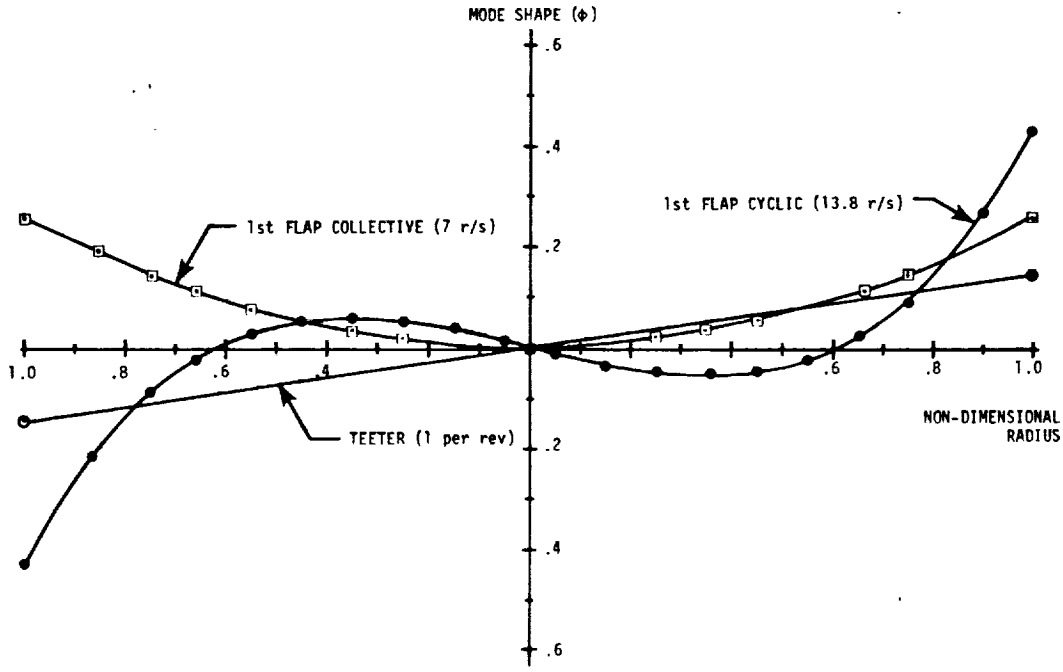

Figure 3. MOD-5A Blade Flapwise Modes

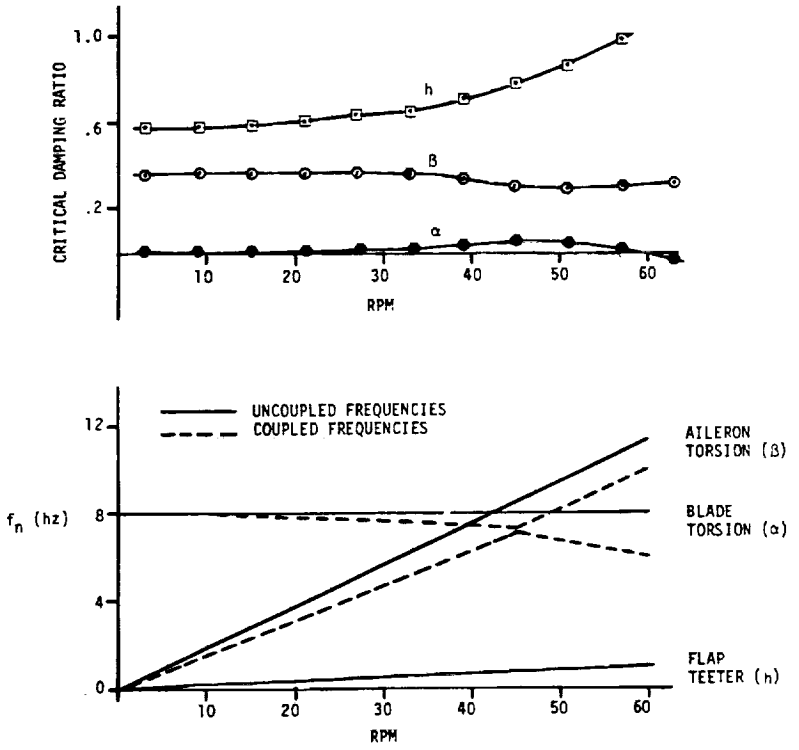

Figure 4a. Flap Teeter Mode Stability
Free Unbalanced Aileron

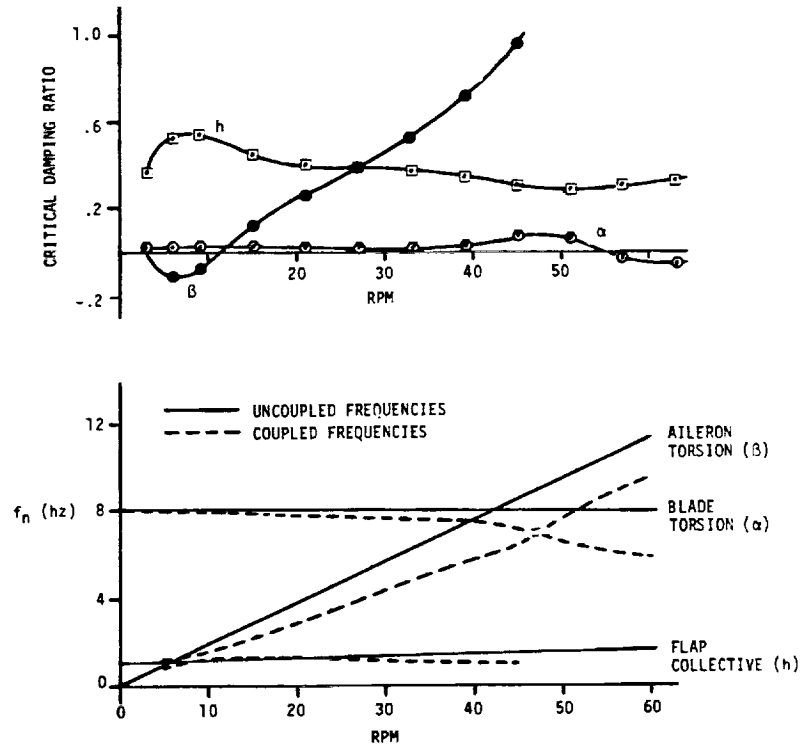

Figure 4b. 1st Flap Collective Mode Stability
Free Unbalanced Aileron

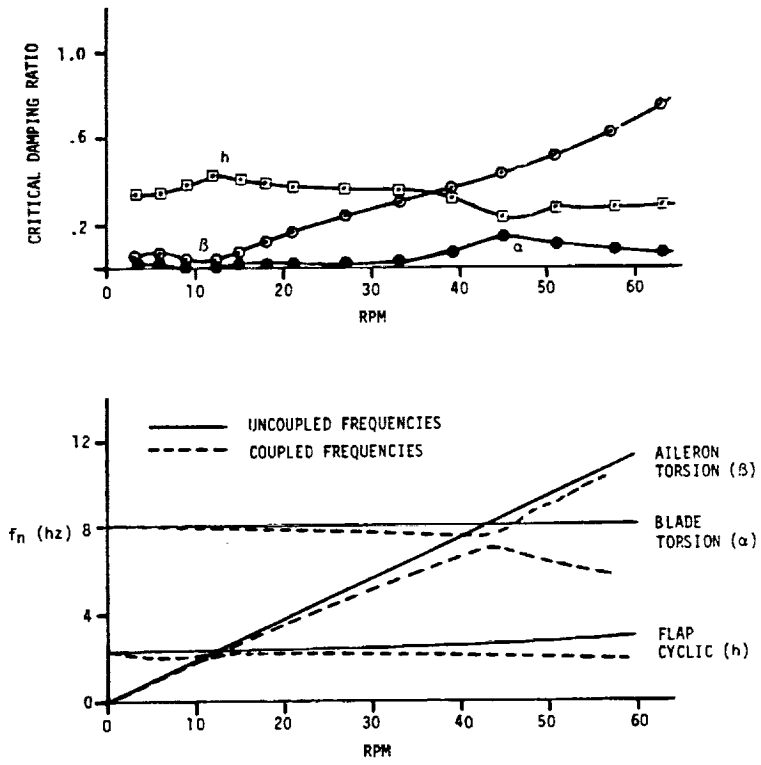

Figure 4c. Flap Cyclic Mode Stability
Free Unbalanced Aileron

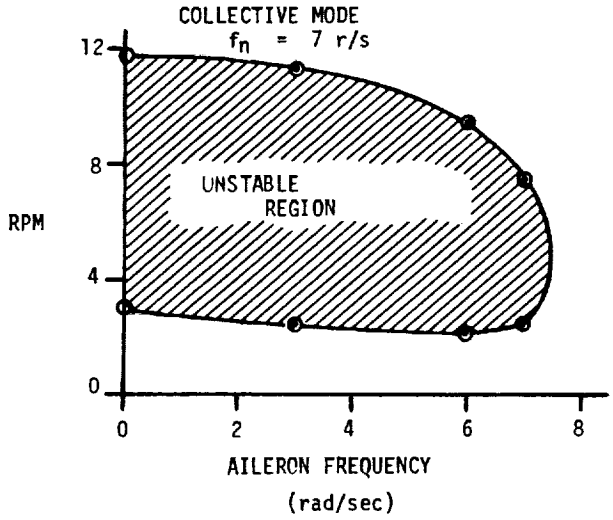

Figure 5. MOD-5A Flutter Boundary - Shown in Terms of Aileron Torsional Frequency

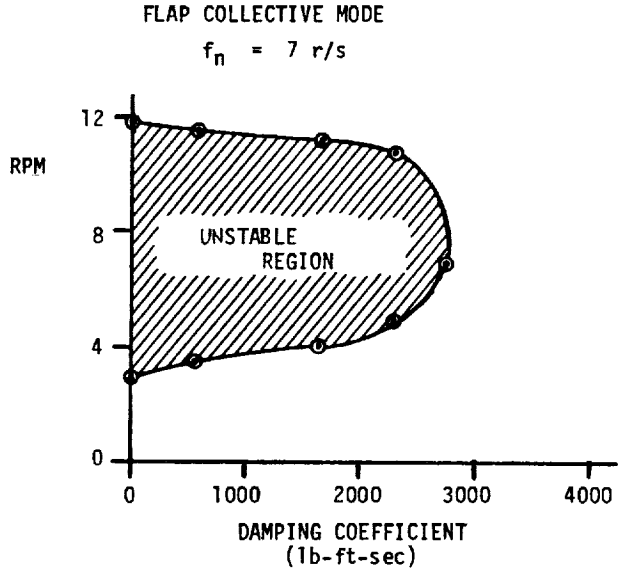

Figure 6. MOD-5A Flutter Boundary - Shown in Terms of Aileron Hinge Damping

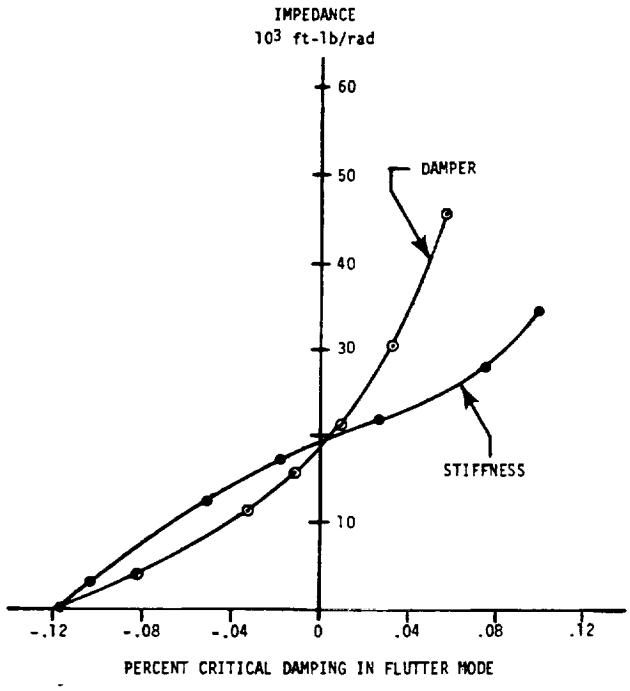

Figure 7. Variation in Modal Damping with Aileron Torsional Impedance, Shown for 6 RPM.

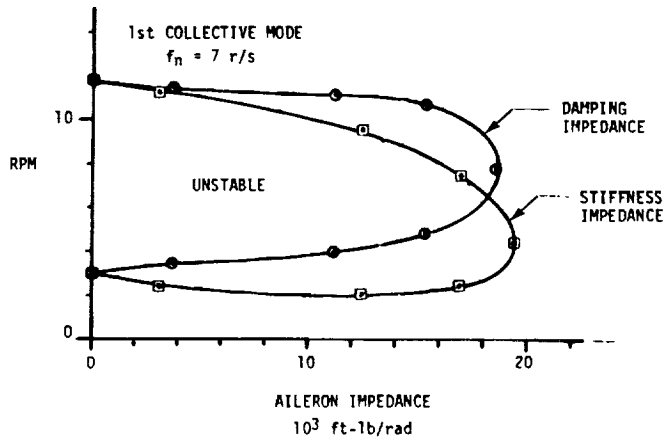

Figure 8. MOD-5A Flutter Boundary Unbalanced Aileron .60R - 1.0R

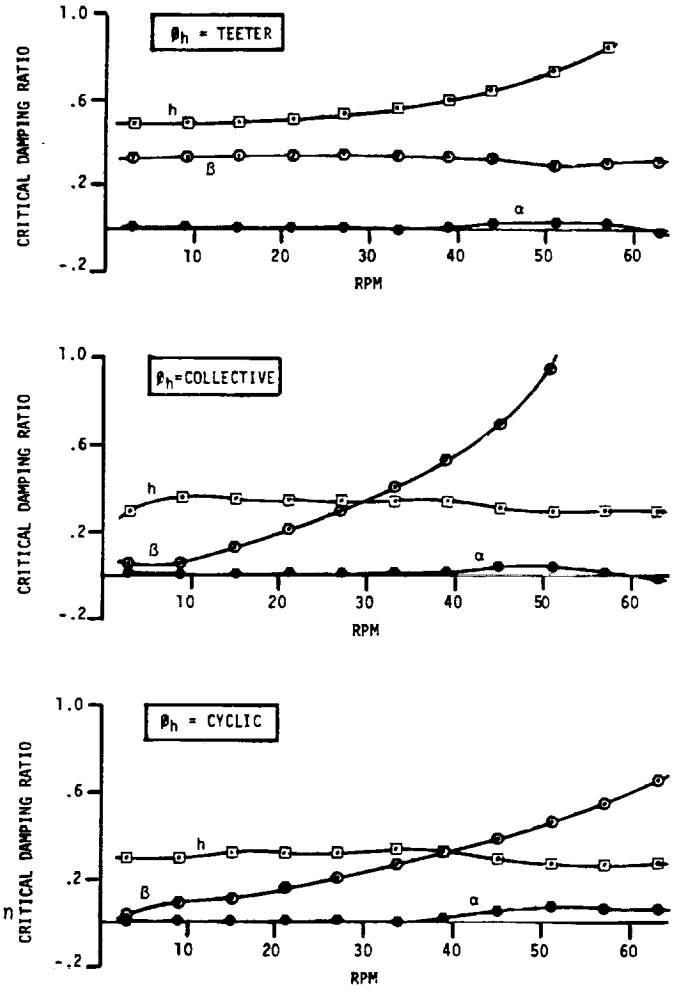

Figure 9. Stability of Free 100% Balanced Aileron .60 - 1.0R

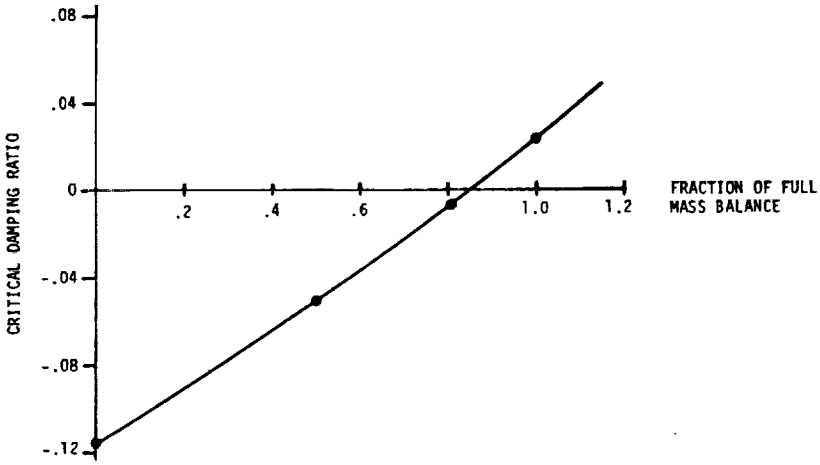

Figure 10. Flutter Damping Coefficient vs. Mass Balance

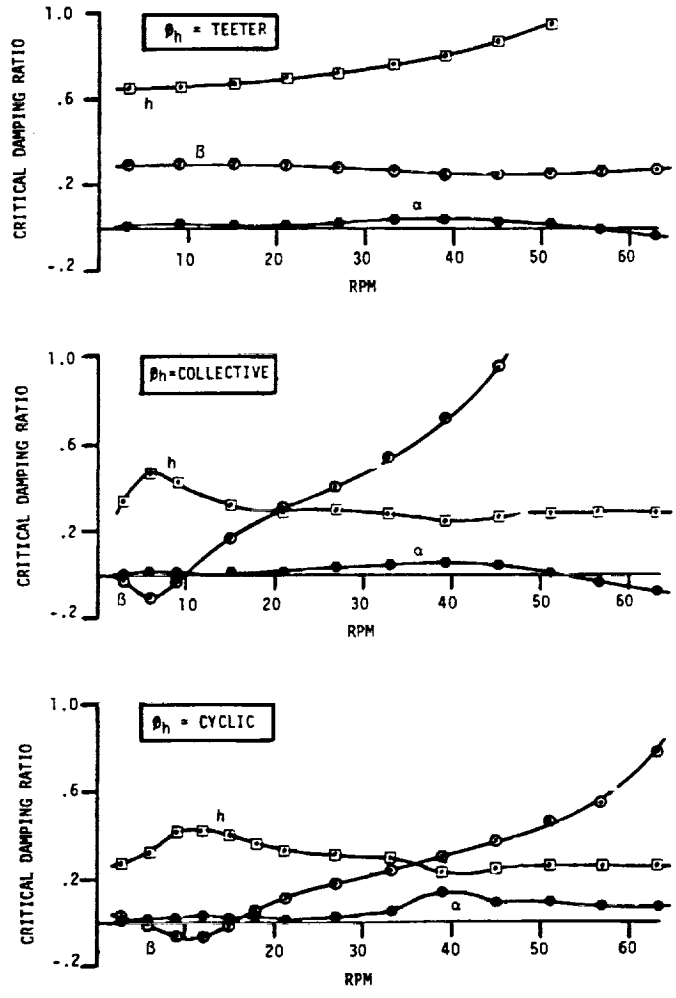

Figure 11. Stability of Free Unbalanced Aileron Extending from .725R - 1.0R

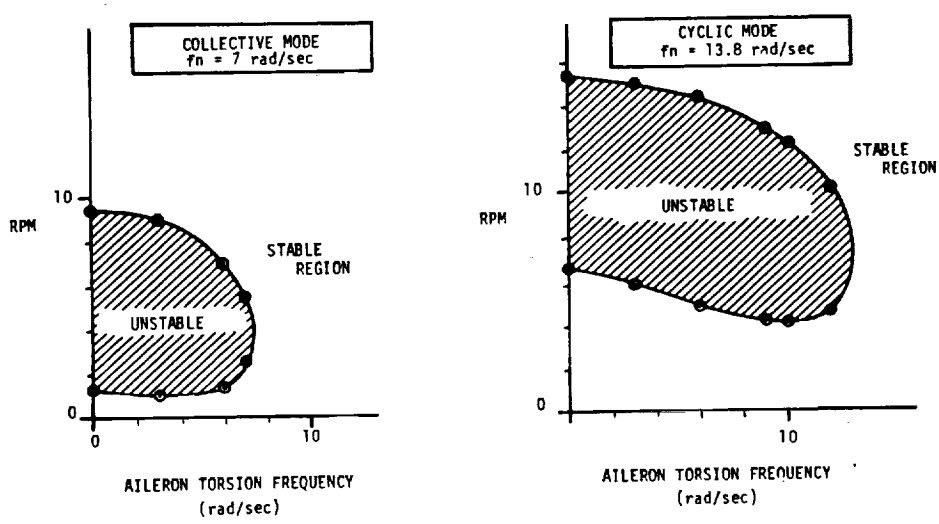

Figure 12. MOD-5A Flutter Boundaries
Unbalanced Aileron .725R - 1.0R
Shown as a Function of Aileron
Torsional Frequency

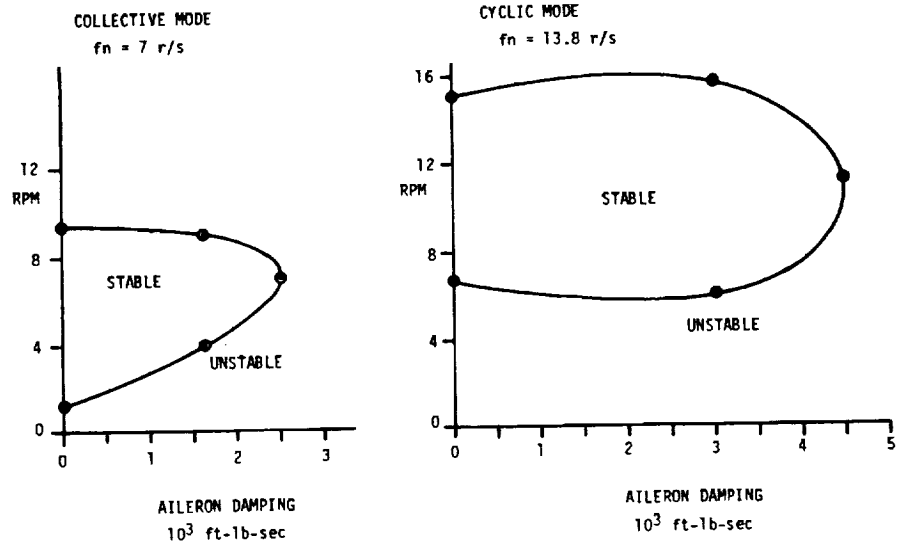

Figure 13. MOD-5A Flutter Boundaries
Unbalanced Aileron .725R - 1.0R
Shown as a Function of Aileron
Damping

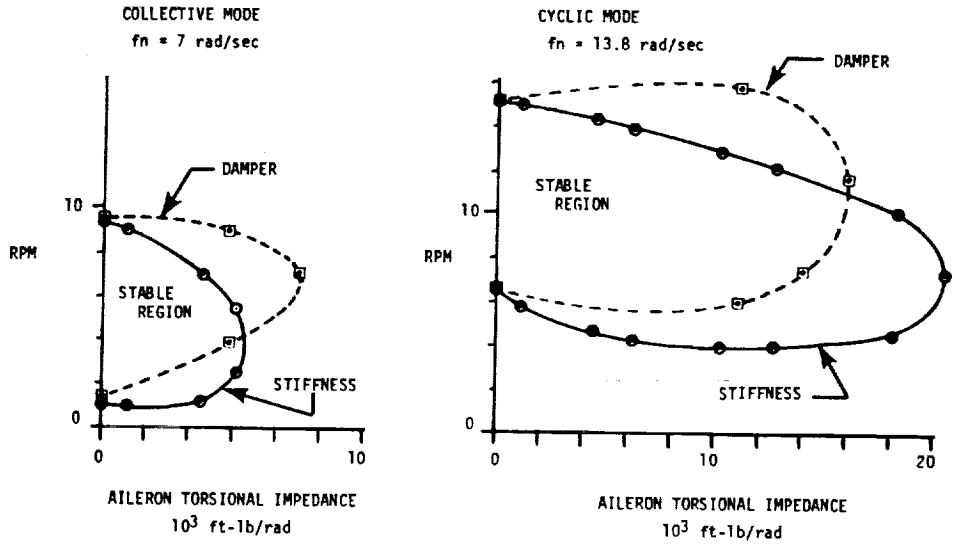

Figure 14. MOD-5A Flutter Boundaries
Unbalanced Ailerons .725R - 1.0R
Shown as a Function of Aileron
Torsional Impedance